ELSEVIER

Computational Materials Science 23 (2002) 283–290

COMPUTATIONAL MATERIALS SCIENCE

www.elsevier.com/locate/commatsci

Effect of applied load on nucleation and growth of γ-hydrides in zirconium

X.Q. Ma [a], S.Q. Shi [a,*], C.H. Woo [a], L.Q. Chen [b]

[a] *Department of Mechanical Engineering, The Hong Kong Polytechnic University, Hung Hom, Kowloon, Hong Kong*
[b] *Department of Materials Science and Engineering, The Pennsylvania State University, University Park, PA 16802, USA*

Accepted 1 June 2001

Abstract

γ-hydride precipitation and growth in zirconium were investigated by using a phase-field kinetic model. The orientation difference of hydride is represented by non-conservative structural field variables, whereas the concentration difference of hydrogen in precipitates and matrix is described by a conserved field variable. The temporal evolution of the spatially dependent field variables is determined by numerically solving the time-dependent Ginzburg–Landau equations for the structural variables and the Cahn–Hilliard diffusion equation for the concentration variable. It is demonstrated that a certain load level is required to completely re-orient hydride precipitates and it is most effective to apply loads during the initial nucleation stage for producing anisotropic precipitate alignment.

1. Introduction

Zirconium and its alloys are primary structural materials in the nuclear power industry. During service, they are susceptible to a slow corrosion process that leads to a gradual pickup of hydrogen impurity from the environment. If the hydrogen concentration reaches the hydrogen solubility limit, hydride will start to form and grow. Because of the brittleness of these hydrides, fracture can initiate at the hydrides depending on the stress level, the distribution and the orientation of hydride. The original strength of the alloy can be reduced by orders of magnitude [1].

Although it was recognized that the shape and distribution of hydrides are critical to hydride induced fracture [2], in situ experimental study of the evolution of hydride morphology is relatively difficult. Most of the observations were made on the surface of the specimen, where the stress state is in plane stress [3]. Some observations were made by sectioning the specimens into the bulk, but this type of observation can only give a "snap shot" of the morphology at a given moment of evolution. The "snap shot" of morphology at the next moment of evolution has to be made by sectioning to a different location in the bulk. In addition, it can be very expensive to study experimentally the morphological evolution of hydride precipitates in irradiated materials because of the cost involved in irradiation protection. Unfortunately, such an expensive test is still the only way to study the

* Corresponding author. Tel.: +852-2766-7821; fax: +852-2365-4705.
E-mail address: mmsqshi@polyu.edu.hk (S.Q. Shi).

0927-0256/02/$ - see front matter
PII: S0927-0256(01)00226-9

evolution of hydride morphology in irradiated materials. A theoretical method capable of predicting a realistic multi-dimensional hydride morphology has not been accomplished, mainly due to the complexity of the analysis. Up to now, computer simulations are based on some idealizations, such as perfect rectangular or elliptical shape of each hydride [4,5]. In most cases, interactions between adjacent hydrides are ignored. On the other hand, computational materials engineering methods have advanced significantly in recent years [6,7]. It is now possible to apply computer simulation to acquire the result that is difficult to obtain in experiments, or to have a better understanding of the mechanism and to predict the properties and morphology of new phases.

A coherent precipitate usually has a number of variants, which are oriented in different but equivalent crystallographic directions and have non-spherical shape since the lattice mismatch between the precipitate phase and the matrix is crystallographically anisotropic. For example, zirconium has a hexagonal close-packed structure. The γ-hydride is formed as a result of high rates of cooling and has a face-centered tetragonal structure. They are platelets parallel to $\{1\,0\,\bar{1}\,0\}$ planes of the matrix. If observed in $(0\,0\,0\,1)$ plane of zirconium matrix, they appear needle-like with axis along three $\langle 1\,1\,\bar{2}\,0\rangle$ directions [8]. During the precipitation process, different variants arrange in such a way that the strain energy caused by the variant is minimized. However, if an external strain or stress is applied during precipitation process, an anisotropic distribution of precipitate variant could be attained and this may result in anisotropic properties of the material.

The oriented hydrides and their precipitation have been studied by a number of researchers [9–11]. They have reported the experimental result of the effect of applied stress on the morphology of hydrides. The results show that in zirconium, the tensile stress tends to change the habit plane in such a fashion that the hydrides orient perpendicular to the tensile stress and that some critical stress might be necessary in order for the hydride to re-orient itself. However, it is not quite clear that in zirconium hydride system the stress-orienting process occurs primarily during nucleation or during variant growth and coarsening. Therefore, the main objective of the present study is to study the stress effect on the nucleation, growth and coarsening process in zirconium hydride system by using computer simulations.

2. Model description

A phase-field kinetic model based on the time-dependent Ginsburg–Landau equation and Cahn–Hilliard diffusion equation was employed. By introducing random noises in the composition and structural order parameter fields, the nucleation of precipitates can be simulated. Therefore, the stress-orienting effects on the selective nucleation, growth and coarsening could be investigated. In the phase-field model, the structural and orientation difference of hydride is represented by non-conservative structural field variables $\eta_1(r,t), \eta_2(r,t), \eta_3(r,t)$, which are called long-range structural order parameter (lro), whereas the concentration of hydrogen in precipitates and matrix is described by a conserved field variable, $C(r,t)$.

According to thermodynamics, the equilibrium state of a multi-phase system corresponds to minimum free energy. The driving force for the temporal evolution of a multi-phase microstructure consists of the following four major contributions: the reduction in chemical free energy; the decrease in the total interfacial energy between different phases; the relaxation of the strain energy caused by the lattice mismatch between the matrix and precipitates; and the reduction in the interaction energy between the initial strain and external load. The simulation will include all these contributions to the total free energy in terms of the field variables, $C(r,t)$ and $\eta_p(r,t)$.

In this work, the local specific chemical free energy is approximated using a Landau-type of free energy polynomial

$$f(C,\eta_p) = \frac{A_1}{2}(C-C_1)^2 + \frac{A_2}{2}(C-C_2)\sum_p^v \eta_p^2 - \frac{A_3}{4}\sum_p^v \eta_p^4 + \frac{A_4}{6}\sum_p^v \eta_p^6$$

$$+A_5\sum_{q\neq p}^{v}\eta_p^2\eta_q^2+A_6\sum_{p\neq q,p\neq r}^{v}\eta_p^4(\eta_q^2+\eta_r^2)+A_7\sum_{p\neq q\neq r}^{v}\eta_p^2\eta_q^2\eta_r^2, \quad (1)$$

where v is the number of orientation variants, C_1 and C_2 are the equilibrium compositions of hydrogen in matrix and in precipitate, respectively; A_1-A_7 are the phenomenological constants which are chosen to fit the local specific free energies as a function of composition for the matrix zirconium and for the hydride.

The interfacial energy between different phases can be expressed through the gradient terms in C and η. The total chemical free energy of an inhomogeneous system may be expressed as

$$F_c=\int_v\left[f(C(\eta_p(r))+\sum_{p=1}^{v}\frac{\alpha_p}{2}(\nabla\eta_p(r))^2+\frac{\beta}{2}(\nabla C)^2\right]d^3r, \quad (2)$$

where α,β are the gradient energy coefficients. The integration is performed over the entire system. Then, the total interfacial energy of the system is defined as the excess free energy associate with the interface, i.e.

$$\sigma=\int\left[f(C,\eta_p)-f_0(C)+\sum_{p=1}^{v}\frac{\alpha_p}{2}(\nabla\eta_p)^2+\frac{\beta}{2}(\nabla C)^2\right]d^3r, \quad (3)$$

where

$$f_0(C)=f(C_\gamma,\eta_{p0}(C_\gamma))+\frac{f(C_\gamma,\eta_{p0}(C_\gamma))-f(C_m,\eta_p=0)}{C_\gamma-C_m}(C_0-C_m), \quad (4)$$

where C_γ and C_m are the hydrogen compositions of the precipitate and matrix, respectively. C_0 is the average composition of the system.

The elastic energy is caused by a lattice mismatch between the precipitate and matrix. According to Khachaturyan's theory, the elastic energy can be expressed as [12]

$$E_{el}=\frac{V}{2}C_{ijkl}\bar{\varepsilon}_{ij}\bar{\varepsilon}_{kl}-VC_{ijkl}\bar{\varepsilon}_{ij}\sum_{p}^{v}\varepsilon_{kl}^0(p)\overline{\eta_p^2(r)}+\frac{V}{2}C_{ijkl}\sum_{p}^{v}\sum_{q}^{v}\varepsilon_{ij}^0(p)\varepsilon_{kl}^0(q)\overline{\eta_p^2(r)\eta_q^2(r)}-\frac{1}{2}\sum_{p}^{v}\sum_{q}^{v}\int\frac{d^3g}{(2\pi)^3}B_{pq}(n)\{\eta_p^2(r)\}_g^*\{\eta_q^2(r)\}_g, \quad (5)$$

where $\overline{(\ldots)}$ represents the volume average of $(\ldots)$, V is the total volume of the system, C_{ijkl} is the elastic constant tensor, ε^0 (p) is the stress-free transformation strain for the pth variant when $\eta_p(r)=1$. Here we can assume $\varepsilon_{ij}^0(r)=\sum\varepsilon_{ij}^0(p)$ $\eta_p^2(r)$, which denotes the local stress-free transformation strain. $B_{pq}(n)=n_i\sigma_{ij}(p)\Omega_{jk}(n)\sigma_{kl}(q)n_l$, where $\Omega_{jk}(n)$ is the reverse matrix of $\Omega_{jk}^{-1}=n_iC_{ijkl}n_l$. $\mathbf{g}$ and $\mathbf{n}=\mathbf{g}/g$ are a reciprocal vector and its unit vector in reciprocal space, respectively. $\{\eta_q^2(r)\}_g$ is the Fourier transform of $\eta_q^2(r)$ and $\{\eta_q^2(r)\}_g^*$ is the complex conjugate of $\{\eta_q^2(r)\}_g$. In the case of whole system subjected to a homogeneous applied strain, $\overline{\varepsilon_{ij}}$ is equal to the applied strain $\overline{\varepsilon_{ij}^a}$ [13].

In the phase-field model, the temporal evolution of the microstructure is determined by solving the time-dependent Ginzburg–Landau equations [14,15] for $\eta_p(r,t)$ and the Cahn–Hilliard diffusion equation [16] for $C(r,t)$:

$$\frac{\partial\eta_P(r,t)}{\partial t}=-L_p\frac{\delta F}{\delta\eta_p(r,t)}+\varsigma_p(r,t),\qquad \frac{\partial C(r,t)}{\partial t}=M\nabla^2\frac{\delta F}{\delta C(r,t)}+\xi(r,t), \quad (6)$$

where L and M are the kinetic coefficients characterizing structural relaxation and diffusion mobility, F is the Helmholtz free energy of the system, $\zeta_p(r,t)$, $\xi(r,t)$ are the Langivin random noise terms which are related to chemical fluctuations in the long-range order parameter and composition, respectively. They satisfy the Gaussian distribution and meet the requirement of the fluctuation–dissipation theorem [17].

Since the above equations are non-linear with respect to field variables, we solve it numerically

with the Fourier Spectral method. In Fourier space, the kinetic Eq. (6) become

$$\begin{aligned}\frac{\partial \eta_p(g,t)}{\partial t} &= -L_p\left\{\frac{\delta F}{\delta \eta_p}\right\}_g + \varsigma_p(g,t),\\ \frac{\partial C(g,t)}{\partial t} &= -Mg^2\left\{\frac{\delta F}{\delta C}\right\}_g + \xi(g,t),\end{aligned} \tag{7}$$

where $\{\ldots\}_g$ is the Fourier transform of $\{\ldots\}$, $\eta_p(g,t)$, $C(g,t)$, $\zeta_p(g,t)$, $\xi(g,t)$ are the Fourier transforms of $\eta_p(r,t), C(r,t)$, $\zeta_p(r,t)$, $\xi(r,t)$, respectively. Eq. (7) can be solved using the semi-implicit Fourier Spectral method [18]. In this method, they can be written as the following:

$$\begin{aligned}&\frac{\eta_p^{n+1}(g)-\eta_p^n(g)}{\Delta t}\\ &\quad= -L_p\left[\left\{\frac{\partial f}{\partial \eta_p}\right\}_g^n + \alpha_p g^2 \eta_p^{n+1}(g)\right.\\ &\qquad\left.+\left\{\frac{\delta E_{\mathrm{el}}}{\delta \eta_p}\right\}_g^n\right] + \varsigma_p^n(g),\\ &\frac{C^{n+1}(g)-C^n(g)}{\Delta t}\\ &\quad= -Mg^2\left[\left\{\frac{\partial f}{\partial C}\right\}_g^n + \beta g^2 C^{n+1}(g)\right] + \xi^n(g).\end{aligned} \tag{8}$$

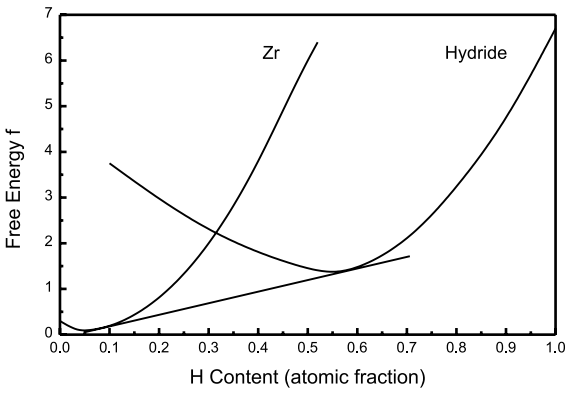

Fig. 1. Specific free energy f for zirconium matrix and γ-hydride as a function of the content of H.

These equations can be solved iteratively to get time-dependence of the field variables and therefore to get microstructural evolution.

3. Simulation results and discussion

We conducted all our simulations in a two-dimensional space with a 512×512 uniform grid. To describe the thermodynamics of precipitation of γ-hydride from zirconium, in the free energy expression (1), we assume that $A_1 = 60, A_2 = -20$, $A_3 = 10, A_4 = 3.5, A_5 = A_6 = A_7 = 0.6$, all in units

Fig. 2. The shape change of γ-hydride sphere particles in the zirconium matrix under the influence of the coherent elastic energy. Each particle was set different initial η_p value.

of mk_BT and $C_1 = 0.05, C_2 = 0.58$. Fig. 1 is a projection of the specific free energy hypersurface on f–C plane for the given parameters. Both gradient energy coefficients were chosen to be 3.5 in units of $mk_BT(\Delta x)^2$, where Δx is the discretizing grid size.

We also assume that the elastic constants of zirconium matrix and precipitate hydride were the same. The elastic constants of zirconium are $C_{11} = 1.5540 \times 10^{12}$, $C_{12} = 0.6803 \times 10^{12}$, $C_{13} = 0.6460 \times 10^{12}$, $C_{33} = 1.7251 \times 10^{12}, C_{44} = 0.3631 \times 10^{12}$, $C_{66} = 0.4409 \times 10^{12}$ erg/cm^3 [19]. A hexagonal to tetragonal transformation of γ-hydride precipitate from zirconium generates three possible equivalent orientation variants. The stress-free transformation strains for the first orientation domains are: 5.70% ([0 0 0 1]), 0.551% ([1 1 $\bar{2}$ 0]), 5.64% ([1 $\bar{1}$ 0 0]) [20]. The strains for the other two orientations were obtained by rotating the first strain by 120° and 240° about c axis, respectively. The kinetic coefficients L_p and M in Eq. (6) were assumed to be 0.4. Reduced time $t^* = t/t_0$ was used

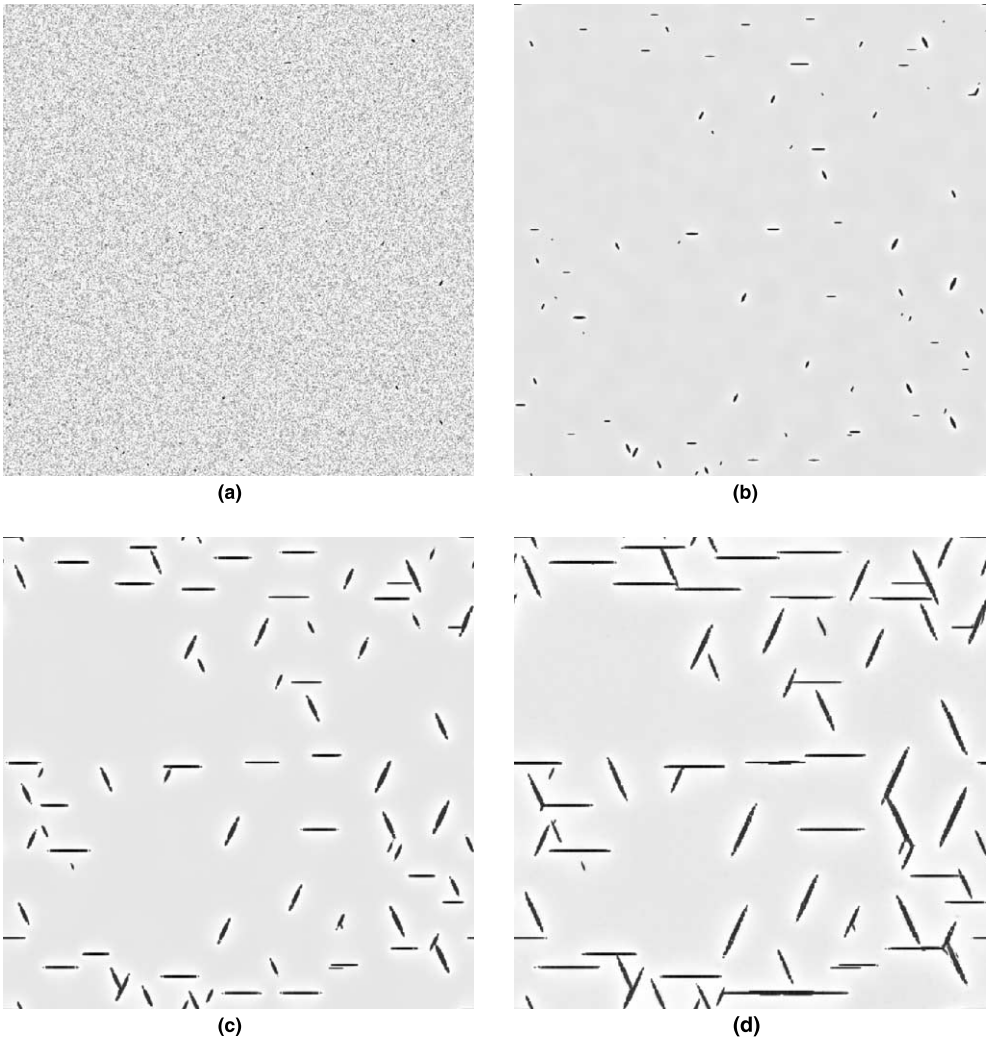

Fig. 3. Simulated precipitation process of γ-hydride from hexagonal zirconium matrix. 512×512 uniform grid: (a) $t^* = 1000$, (b) $t^* = 2000$, (c) $t^* = 4000$, (d) $t^* = 6000$.

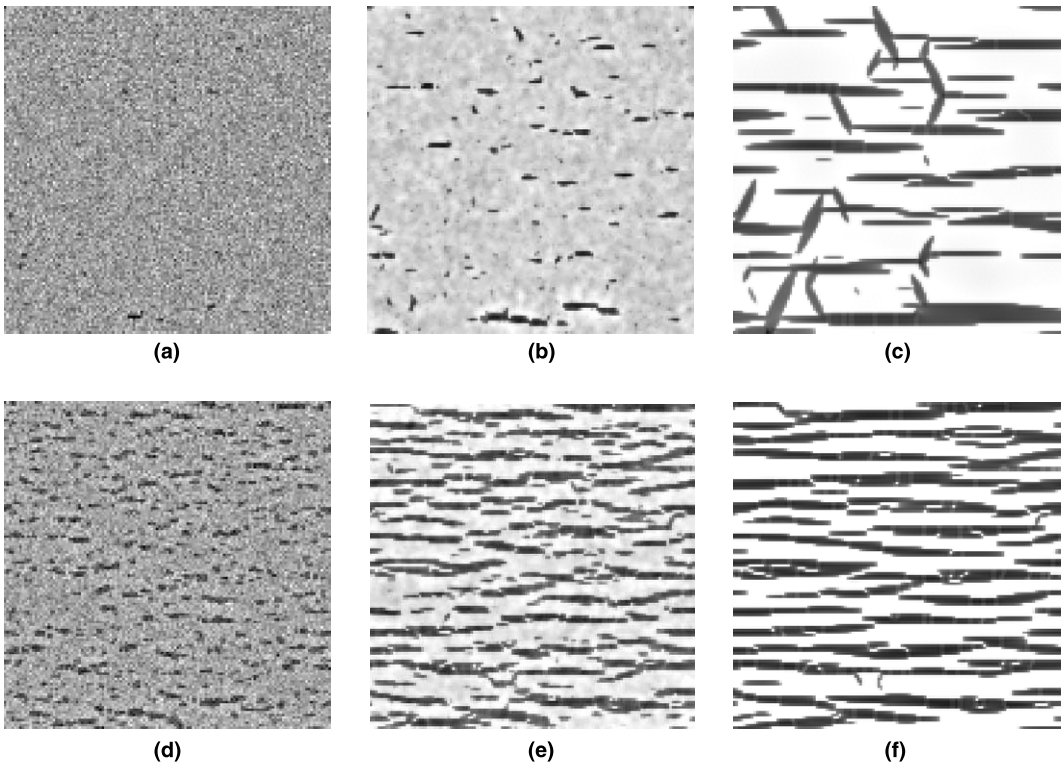

Fig. 4. γ-hydride precipitation under external load applied vertically. Load applied both in nucleation and growth process. $[1\,1\,\bar{2}\,0]$ direction of the matrix is along horizontal axis, 128×128 uniform grid: (a) strain = 0.14%, $t^* = 500$; (b) strain = 0.14%, $t^* = 1000$; (c) strain = 0.14%, $t^* = 5000$; (d) strain = 0.42%, $t^* = 500$; (e) strain = 0.42%, $t^* = 1000$; (f) strain = 0.42%, $t^* = 5000$.

to represent the aging time, here $t_0 = (Lmk_BT)^{-1}$. For each iteration, the time step is $\Delta t^* = 0.0008$.

The morphology of a coherent precipitate affects the properties of the materials. Therefore, it is important to know how the precipitate shape evolves during nucleation and aging process. In order to investigate the morphological evolution of a hydride particle in zirconium matrix, we embedded three spherical hydride particles in the matrix. The composition of three hydride particles is 0.58 and that of the matrix is 0.1. The lro values (η_1, η_2, η_3) within each particle were set (1.0, 0.0, 0.0), (0.0, 1.0, 0.0), and (0.0, 0.0, 1.0), respectively. It was observed that particles changed their shapes from circles to thin needles during the aging process and each circle grew along different directions. The evolution process is shown in Fig. 2. The shape change of the particles is due to the crystallographical anisotropy of transformation strain of the particle. The morphology of a coherent precipitate is actually determined by the balance between the strain energy and interfacial energy. Since the interfacial energy was assumed to be isotropic, the shape change here is mainly caused by the elastic energy, which is a function of shape and orientation of the precipitates. It is obvious that their morphology is dominated by the elastic energy.

In order to simulate nucleation process, all the initial values of $C_0(r,t)$ were set to be 0.1, all $\eta_p(r,t)$ to be zero and two noise terms in Eq. (6) were turned on during the first 1000 time steps to simulate the local thermal fluctuations of $C(r,t)$ and $\eta_p(r,t)$. It can be seen from Fig. 3(a), during the nucleation process, that there were some nuclei larger than the critical size formed in some places. In the growing process, these nuclei grow along habit plains with an angle of about 120° from each

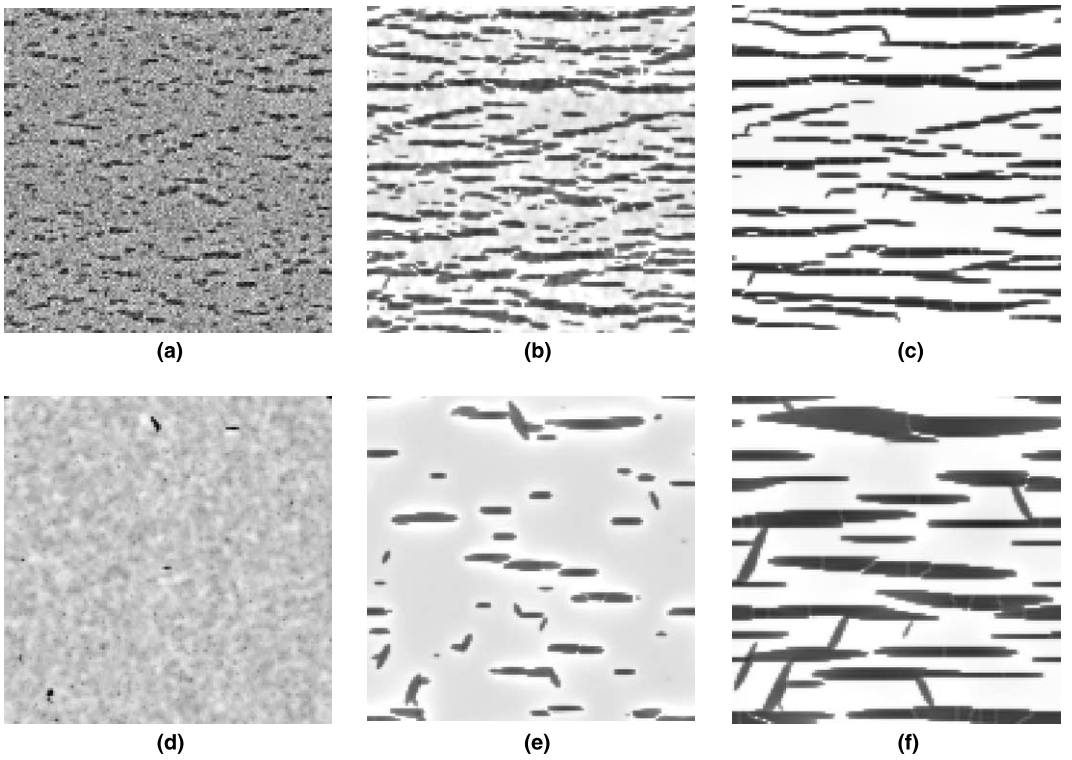

Fig. 5. Microstructural evolution under different constant conditions. $[1\,1\,\bar{2}\,0]$ direction of the matrix is along horizontal axis. External load applied vertically, 128×128 uniform grid, strain = 0.42%. (a)–(c) Constrained nucleation followed by free variant growth. (a) $t^* = 500$, (b) $t^* = 1000$, (c) $t^* = 5000$. (d)–(f) Free nucleation followed by constrained variant growth. (d) $t^* = 1000$, (e) $t^* = 2000$, (f) $t^* = 5000$.

other. In a multi-variant system, the growth of different precipitate variants and their mutual positions is strongly affected by long-range elastic interactions between the variants. The morphology of the hydride precipitates in zirconium obtained from the computer simulation agrees well with that of the TEM observations of Bailey (see [8, Figs. 5(a) and 6(b)]).

To investigate the effect of externally applied load on the growth of hydride a tensile load was initially exerted on the hydrogen-zirconium system to generate a constant constraint strain. Under such a constraint strain, the precipitates that are in the habit plane perpendicular to the tensile stress grow preferentially. The simulations were taken under different levels of the applied load. The simulation result is shown in Fig. 4. From the result it can be seen that the larger the applied stress, the more strongly the precipitates aligned along the habit plane perpendicular to the applied load growth. When the applied strain reached 0.42%, only the variant perpendicular to the applied load remained and the variants of the other two directions disappeared, forming parallel alignment of the precipitates. This indicates that applied load has a strong effect on the orientation of the variant. The precipitates are distributed in such a way that the elastic energy is minimized. The result also shows that the larger the applied tensile load, the higher the nucleation rate would be. This is consistent with the fact that while the applied load suppresses the nucleation of certain variants, it increases the driving force for nucleation for the remaining variants.

We have also studied how the applied stress affects the orientation of variants, and whether it

has a strong effect during the nucleation stage or growth stage. In our simulation, we applied tensile strains at the nucleation stage and then removed it during growth and coarsening period, or vice versa. The results are shown in Fig. 5. From (a)–(c) are under the condition of constraint nucleation under 0.42% at initial 1000 time steps followed by free variant growth. From (d)–(f) are the results of free nucleation and constrained growth under 0.42%. Compare the result of Figs. 5((a)–(c)) and 4((d)–(f)), if the load is applied above some magnitude at the nucleation stage and removed it during growth, the hydrides tend to align parallel, similar to the result of applying load during both the nucleation and growth stages. From Figs. 5((d)–(f)) we can see that free nucleation followed by constraint growth at the same load level, the degree of alignment is not as strong as the constraint nucleation case. This demonstrates that it is most effective to apply stresses during the initial nucleation stage for producing anisotropic precipitate alignment. This is understandable from the elastic interactions among the variants, and the elastic interaction between the coherent stress and the applied stress field. At the nucleation stage, the interactions among the different variants are weak, so the applied stress field plays a major role. Since the hydride in zirconium has a positive mismatch strain, the nuclei of the precipitate tend to grow along the direction perpendicular to that of tensile stress so as to lower their energy.

4. Conclusion

Precipitation and growth of γ-hydrides in zirconium matrix with or without applied stress were investigated using a phase-field kinetic model. The following simulation results were obtained:

- The morphology of the precipitate is mainly determined by the strain energy of the system.
- Without external load, our simulation predicts three equivalent orientations of γ-hydrides, which is consistent with TEM observations.
- Under the influence of applied load, the distribution of hydride becomes anisotropic, and hydrides align perpendicular to the direction of the applied tensile load.
- A certain load level is required to completely reorient hydride platelets.
- It is most effective to apply loads during the initial nucleation stage for producing anisotropic precipitate alignment.

Acknowledgements

This work was supported by grants from the Research Grants Council of Hong Kong (B-Q411) for Shi, Woo and Chen, and from Hong Kong Polytechnic University (G-V851) for Ma, and from the U.S. National Science Foundation (DMR 96-33719) for Chen.

References

[1] L.A. Simpson, C.D. Cann, J. Nucl. Mater. 87 (1979) 302.
[2] S.-Q. Shi, M.P. Puls, in: A.W. Thompson, N.R. Moody, (Eds.), Hydrogen Effects in Materials, published by TMS, 1996, pp. 611–621.
[3] S. Sagat, S.Q. Shi, M.P. Puls, Mater. Sci. Eng. A 176 (1994) 237–247.
[4] S.Q. Shi, M.P. Puls, J. Nucl. Mater. 208 (1994) 232–242.
[5] S.Q. Shi, M.P. Puls, S. Sagat, J. Nucl. Mater. 208 (1994) 243–251.
[6] R. Dierk, Computational Materials Science: The Simulation of Materials Microstructures and Properties, Weinheim, New York, 1998.
[7] D.Y. Li, L.Q. Chen, Acta Materialia 46 (1998) 2573.
[8] J.E. Bailey, Acta Metal. 11 (1963) 267.
[9] G.P. Walters, Electrochem. Tech. 4 (1966) 216.
[10] W.J. Babyak, Trans. AIME 239 (1967) 252.
[11] S.Q. Shi, Scrip. Mater. 41 (1999) 1115.
[12] A.G. Khachaturyan, Theory of Structural Transformations in Solids, Wiley, New York, 1983.
[13] D.Y. Li, L.Q. Chen, Acta Mater. 45 (1997) 2435.
[14] J.W. Cahn, J.E. Hilliard, J. Chem. Phys. 28 (1958) 258.
[15] Y. Wang, L.Q. Chen, A.G. Khachaturyan, J. Am. Ceram. Soc. 76 (1993) 3029.
[16] S.M. Allen, J.W. Cahn, Acta Metall. 27 (1979) 1085.
[17] E.M. Lifshitz, L.P. Pitaevskii, Statistical Physics, Pergamon Press, Oxford, 1980.
[18] L.Q. Chen, J. Shen, Comput. Phys. Commun. 108 (1998) 147.
[19] M. Lgarashi, Phil. Mag. B 63 (1991) 603.
[20] G.J.C. Carpenter, J. Nucl. Mater. 48 (1973) 264.